Modeling of a Hybrid Controller for Electric Vehicle Battery Charging Using Photovoltaic Panels

Marius-Alexandru DOBREA[1]*, Sergiu-Stelian ILIESCU[1,2], Nicoleta ARGHIRA[1], Mihaela VASLUIANU[3]

[1] Faculty of Automatic Control and Computer Science, University Politehnica of Bucharest, 313 Splaiul Independentei, 060042 Bucharest, Romania
marius.alexandru.dobrea@gmail.com (**Corresponding author*), nicoleta.arghira@upb.ro

[2] Technical Sciences Academy of Romania – ASTR, 26 Dacia Avenue, 030167 Bucharest, Romania
iliescu.shiva@gmail.com

[3] Faculty of Hydrotechnics, Technical University of Civil Engineering of Bucharest, 124 Lacul Tei Avenue, 020396 Bucharest, Romania
mihaela.vasluianu@utcb.ro

Abstract: The present paper introduces a novel approach for voltage control during the charging and discharging of a battery of an electric vehicle. The control algorithm joins a conventional PID controller together with a Fuzzy-PID controller, in order to compute the command signal. The effectiveness evaluation of the control algorithm is computed by simulation and tested in the context of charging a battery using solar energy harnessed from photovoltaic (PV) panels. This hybrid approach employs a Phase-Shifted Full-Bridge (PSFB) converter as actuator. By comparing the step response of the charging process of the PID controller with the response of the proposed hybrid controller, improved results were obtained in terms of performance for the latter one.

Keywords: Photovoltaic panel, Phase-Shifted Full-Bridge converters, PID controller, Fuzzy-PID controller, Electric vehicle, Battery charging.

1. Introduction

Over the past ten years, photovoltaic (PV) systems have rapidly become a major source of renewable energy worldwide. This is due to their ability to be used in a wide range of applications, from small off-grid systems in rural areas to large power plants that are connected to the grid. Photovoltaic systems can be installed on rooftops, fields or other structures, making them a flexible and scalable option for generating electricity (Maher et al., 2023).

Understanding photovoltaic systems for exploitation initially requires grasping the functioning principle of the photovoltaic cell. The power of a solar cell typically ranges from 1 to 3 W, (Bhukya et al., 2022). PV panels composed of such cells integrate into PV power plants for residential systems ranging 3-20 kW or commercial systems going up to several megawatts (Andronic et al., 2023). In the case of a photovoltaic system, a fuzzy controller can be applied to optimize the electricity production and ensure more efficient operation. PV systems are exposed to variations in sunlight, temperature, and other factors that can affect the electricity production. The fuzzy controller can automatically adjust the parameters of the photovoltaic system, in order to achieve the best performance under varying conditions.

The benefits of applying a fuzzy controller to a photovoltaic system include adaptability to changing environmental conditions, resistance to disturbances, and the ability to enhance system performance. In practice, such a control system can prove to be more efficient compared to traditional control methods, especially when there are uncertainties or unforeseen changes in the operating environment of a photovoltaic system.

Often, a PID (proportional integral derivative) controller can be combined with a fuzzy controller, with the classical control part ensuring fine control over specific parameters, while the fuzzy controller handles adaptability and resistance to environmental variability (Maher et al., 2023).

Other methods for maximum power point tracking involving artificial intelligence algorithms can be deployed (Alshareef, 2022). The delays introduced by computational time delay show the necessity to consider a hybrid approach for the PV system control solutions.

An efficient energy system is one where the supply and demand are situated close together. Since electrical vehicles are becoming more used nowadays, these are important loads of the residential or commercial energy consumers (Stamatescu et al., 2020). So, solutions for charging electrical vehicles from photovoltaic power are studied lately.

https://doi.org/10.24846/v32i4y202303

Control for a hybrid electric vehicle using a neural network controller with a radial basis function is proposed in (Ravipati et al., 2021). The controlled variable is the input voltage of the DC (direct current) motor which further is used for speed regulation with a PI (proportional integral) controller. The energy sources for supplying the hybrid vehicle are PV panels as well as a fuel cell. However, the computation time for the neural controller is a downside of this approach.

Charging automotive batteries using a photovoltaic (PV) system is a very useful, convenient, and environmentally friendly application. It involves using solar energy to power a charger that will recharge the batteries of the vehicle, allowing to fuel the car using clean and renewable energy.

It represents a sustainable and efficient method of obtaining electrical energy for vehicles, especially in areas with abundant sunlight. This type of system is often referred to as an “off-grid PV system for electric vehicle charging” or an “on-grid PV system with storage for electric vehicles” (Dobrea et al., 2020).

It is important to mention that the charging performance depends on several factors, such as the power of the photovoltaic panels, battery capacity, duration of sun exposure, and weather conditions. On sunny days, a properly sized PV system and suitable batteries should be able to charge automotive batteries for nighttime use or during periods when the panels do not produce sufficient electrical energy.

In (Leijon & Boström, 2022), the authors presented various charging strategies for multiple types of electric vehicles. The authors concluded that the most suitable charging strategy for an electric vehicle in the near future depends on the timing and location of the charging, the vehicle type, and its usage.

The authors Mohamed et al. (2022) developed a system for charging electric vehicles with minimal costs, using a photovoltaic system isolated from the national electricity grid to avoid disconnection from the grid.

This study was conducted on five different types of vehicles. The simulation was accomplished using variations of solar radiation from 600 W/m2 to 1000 W/m2 and temperatures ranging from 20°C to 30°C, implemented in MATLAB software. The results indicate that the charging time for the five types of electric vehicles falls within the range predicted in the electric vehicles database.

A PV system was designed in (Tauš et al., 2020) to support the charging of electric vehicles. The authors created an optimized model for a PV system with batteries, based on real vehicle consumption data, actual daily travelled distance, location, and the time of coverage during adverse weather conditions. The entire system design was accomplished through simulations conducted over the course of a year. The authors analyzed the interrelationships for calculating the performance of a photovoltaic system, based on the daily consumption of the electric vehicle and the time required to overcome unfavorable weather.

This article proposes a new hybrid voltage regulator for the process of charging electric vehicle batteries, based on the results and previous research from (Dobrea et al., 2021). This hybrid controller consists of a PID part and a fuzzy controller. It is intended to be used in situations where the energy generated by the photovoltaic panels is used for charging electric vehicles batteries.

Section 2 describes the modeling of a Phase-Shifted Full-Bridge converter. Section 3 details the implementation of a system comprising a PID and a Fuzzy-PID controller. Section 4 performs the adjustment of a battery using the proposed hybrid system. Section 5 depicts the conclusions.

2. Modeling of DC-DC Converters

Two distinct categories for DC-DC converters can be differentiated: isolated and non-isolated.

In the PV systems, most used converters are non-isolated. These converters can be also divided into BOOST, BUCK, and simple primary-inductor converter (SEPIC) (Koç et al., 2022).

The boost converter is prevalent used and finds multiple applications, particularly in identifying the maximum power point for photovoltaic panels, thanks to its simple design and fast response.

To determine the maximum power point, a flexible and fast-response algorithm is required, and the most frequently used methods to track it are known as fuzzy logic, incremental conductance and perturb and observe, as validated in (Hai, Zhou & Muranaka, 2022).

$$\frac{V_0}{V_i} = \frac{T_s}{T_{off}} = \frac{1}{1-D} \tag{1}$$

where T_s is the switching period, D is the duty cycle, and T_{off} stands for the transistor turn-off time or switch-off period.

Regarding the operating mode of the boost converter, Koç et al. (2022) mention that it can operate in two distinct modes: discontinuous conduction mode and continuous conduction mode, depending on the energy storage capacity and the relative switching interval.

On the other hand, isolated DC-DC converters represent another distinct category, resulting from non-isolated ones by adding transformers and rectifying circuits on the output.

These isolated converters offer advantages, including a higher conversion rate of voltage compared to conventional topologies, as demonstrated in the examples from (Kim et al., 2021).

In battery charging applications, isolated DC-DC converters that are based on buck converter are recommended. These include push-pull, forward, full-bridge and half-bridge converters. Further, a comparison is depicted in Table 1 for the common isolated step-down DC-DC converters, based on their parameters: switch voltage, switch current, number of switches and frequency. The notations in the table are as follows: I_o is the output current, f_s is the switching frequency and n represents the transformer winding ratio.

Table 1. Converters with galvanic isolation

Converter	Switch Voltage	Switch Current	No. of Switches	Switch Frequency
Push-pull	$2*V_{in}$	$I_0 / (2*n)$	2	$2*f_s$
Simple forward	$2*V_{in}$	I_0 / n	1	f_s
Double forward	V_{in}	I_0 / n	2	f_s
Half-bridge	V_{in}	I_0 / n	2	$2*f_s$
PSFB	V_{in}	$I_0 / (2*n)$	4	$2*f_s$

Phase-Shifted Full-Bridge Converters (PSFB Converters) represent an important class of electric power conversion devices. These converters can transform direct current voltage to higher or lower levels, finding various applications in power supply systems, renewable energy sources, and electric motor drives.

PSFB converters are composed of a bridge formed by four semiconductor devices and four diodes, arranged in a specific manner. The four semiconductor devices are typically IGBT (insulated-gate bipolar) or MOSFET (metal-oxide-semiconductor field-effect) transistors, chosen for their superior performance in high-power applications. The bridge configuration completes the circuit for converting electrical energy between the input and output voltage.

The operating principles of PSFB converters are based on how the transistors and diodes are controlled to achieve the desired output voltage. Bidirectional current control allows both up and down regulation of the output voltage, making these converters highly versatile (Mendoza-Varela et al., 2021).

Typically, the converters are controlled using pulse width modulation (PWM) techniques. This technique involves generating a series of voltage pulses with variable durations, and the ratio between the on-time (when the transistor is open) and off-time (when the transistor is closed) determines the average output voltage.

Figure 1 shows a simplified circuit of a PSFB converter. The MOSFET switches are building the full bridge on the primary side of transformer T_1. Q_1 and Q_2 have a 50% duty cycle and a 180 degrees phase difference in between each other. Switches Q_3 and Q_4 operate in the same way as Q_1 and Q_2.

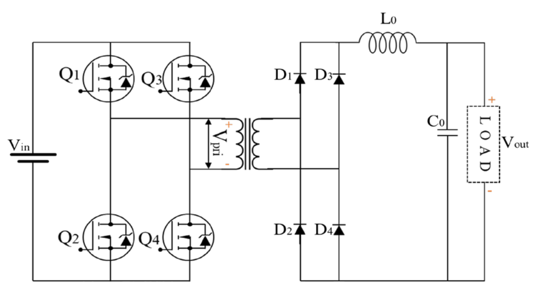

Figure 1. Structure of a PSFB converter (Mendoza-Varela et al., 2021)

The Pulse Width Modulation switching signals for the Q_3 - Q_4 connection of the full bridge are phase-shifted compared to the signals for the Q_1 - Q_2 connection. The transferred energy is determined by the overlap of the signals between the diagonal switches, and this is influenced by the value of phase shift, as show in Figure 2.

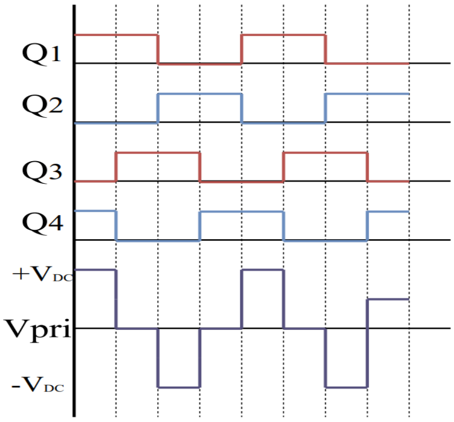

Figure 2. Switching control signals

The diodes ensure the rectification of the current doubler in the transformer secondary side. The inductor and capacitor operate as output filters.

The LR inductor helps to resonate the transformer leakage inductance with the MOSFET capacitance, which eliminates the switching voltage and improves circuit efficiency.

The voltage V_{Lo} is applied to the output inductor L_o it is calculated as follows:

$$V_{L_0} = nV_{in} - V_{out} \quad (2)$$

The operation of the converter is expressed as voltage transfer as follows:

$$V_{L_0} \cdot DT_s = n\left(V_{in} - V_{out}\right) \cdot DT_s = V_{out}\left(\frac{T_s}{2} - DT_s\right) \quad (3)$$

where the phase shift of the PSFB converter is represented by D and Ts is the sampling period (Yao et al., 2022).

Figure 3 represents the implementation of a PSFB DC-DC converter for battery bank charging. The input voltage is approximately 400 V, and the output voltage is 48 V. The switching frequency is 50 kHz, and the current ripple has a value of 20%. The maximum output voltage represents a 15% margin from the nominal voltage and has a value of 55 V. The ratio of the transformer is 0.1375.

Figure 4 shows the switching waveforms for the implemented system. It consists of generating rectangular pulses with a constant voltage level (V_1) during the on-time (T_{on}) and a zero voltage level during the off-time (T_{off}). As a result, the average output voltage (V_{out} = 48 V) can be adjusted by modifying the $T_{on}/\left(T_{on}+T_{off}\right)$ ratio.

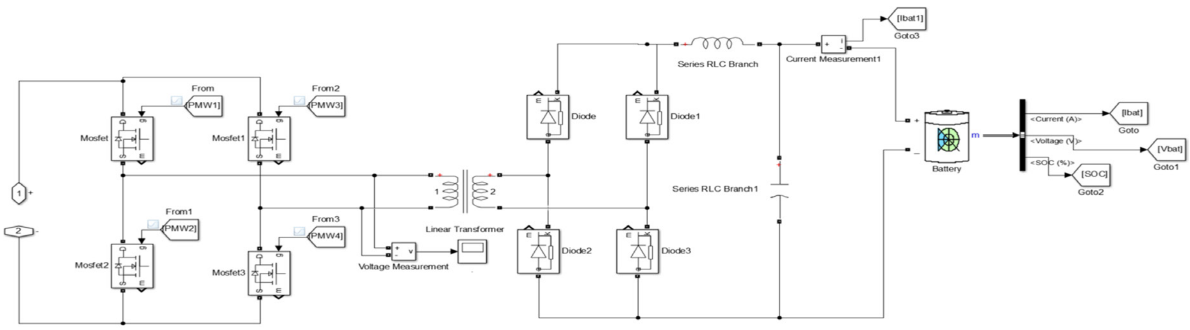

Figure 3. Simulink model of a PSFB converter

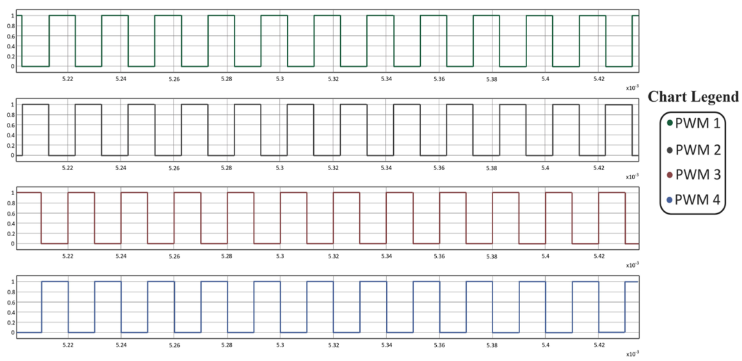

Figure 4. Simulation of switching waveforms of PWM in SIMULINK

3. The Tunning of the Hybrid Controller

This controller for the electric vehicle battery voltage is further proposed. The actuator in the control system is the PSFB converter. For the actuator, the input variable is a PWM signal and the output variable is the battery voltage.

A PSFB DC-DC converter is itself a complex system, and the control requirements for optimal battery charging are high.

Using traditional PID controllers can be susceptible to noise and disturbances in the system. Abrupt variations or noise in the measurement signals can lead to errors in regulation and undesired oscillations in the output.

Additionally, external disturbances can affect the regulation performance, often requiring additional filtering or special processing to eliminate them.

While a PID (proportional-integral-derivative) control might offer decent control under certain conditions, adding fuzzy logic can significantly improve performance.

The present study proposes the development of a hybrid system composed of two distinct types of controllers: a Fuzzy-PID controller and a traditional PID controller, as show in Figure 5.

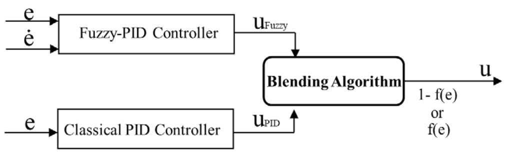

Figure 5. Structure of the hybrid controller

The controller input variables correspond to the voltage error, along with its error gradient. Both the Fuzzy-PID and classical PID controllers generate control values (U_{Fuzzy} and U_{PID}) for the actuator.

These control values are combined in an algorithm, and the result is the final control value transmitted to the PSFB actuator.

While the traditional PID controller acts solely based on the error, integral of the error, and its derivative as an input variable, the Fuzzy-PID controller supervises two input parameters: the error and the derivative of the error, as it can be seen in Figure 6.

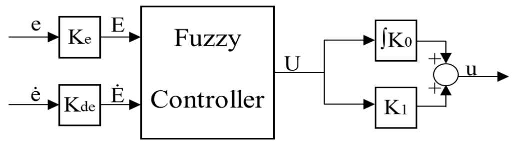

Figure 6. Design of a Fuzzy-PID controller

The Fuzzy-PID controller incorporates a control strategy based on fuzzy logic. It extends the monitoring and evaluation capability of the system by including two input parameters: the error and the derivative of the error.

Using fuzzy logic allows handling imprecise and ambiguous information, providing a higher degree of adaptability and resistance to variations and uncertainties (Baral et al., 2023).

In the present study, the output variable is modelled with singleton membership functions and triangular membership functions are implemented for the input variables, as illustrated in Figure 7.

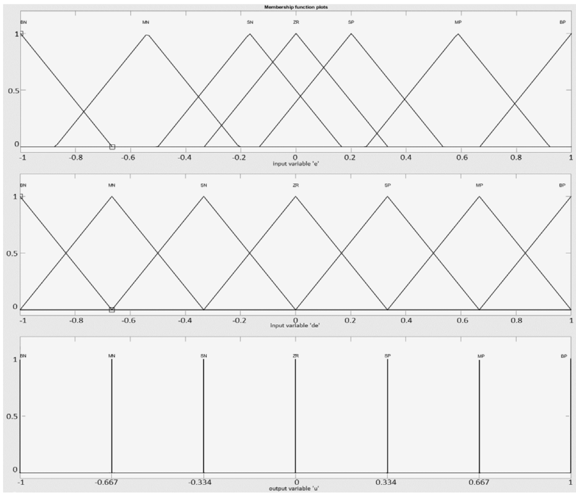

Figure 7. Proposed membership functions of the Fuzzy-PID controller

The seven membership functions for the variables are as follows: BN (Big Negative), MN (Medium Negative), SN (Small Negative), ZR (Zero), SP (Small Positive), MP (Medium Positive), and BP (Big Positive).

The intervals for triangular input signals (error) were determined through an experimental analysis in relation to the output signal, implicitly with the battery voltage, by successive iterations until the optimal values were determined.

Initially, the fuzzy system membership functions were implemented as 7 triangular signals with equal distribution. The output membership functions were declared and the rule base was created through a linear distribution. The identification of the triangular input limits was determined after several experimental tests, considering minimal voltage oscillation index.

The Fuzzy-PID controller is composed of a rule base consisting of 49 rules arranged in a matrix with 7 rows and 7 columns, as shown in Table 2. By applying the rule base, the resulting control surface can be visualized in Figure 8.

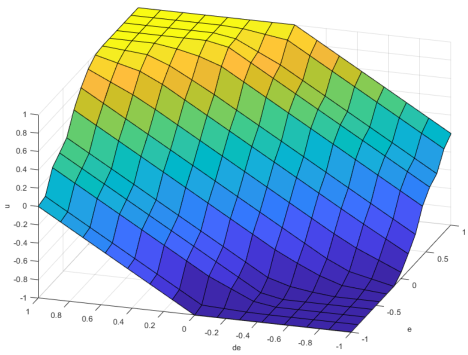

Figure 8. The control surface of the controller

Table 2. Rule Base for Fuzzy-PID Controller

$E/\dot{E}$	BN	MN	SN	ZR	SP	MP	BP
BP	ZR	SP	MP	BP	BP	BP	BP
MP	SN	ZR	SP	MP	BP	BP	BP
SP	MN	SN	ZR	SP	MP	BP	BP
ZR	BN	MN	SN	ZR	SP	MP	BP
SN	BN	BN	MN	SN	ZR	SP	MP
MN	BN	BN	BN	MN	SN	ZR	SP
BN	BN	BN	BN	BN	MN	SN	ZR

A combination of a classical PID controller and a Fuzzy-PID controller is further proposed, using a blending algorithm based on a specific function of the control error.

In the initial stage, the algorithm determines which of the two control structures, either the classical PID controller or the Fuzzy-PID controller, dominates the process control.

The outputs generated by the Fuzzy-PID controller and the classical PID controller are weighted using the weighting functions 1-f(e) and f(e).

These weighting functions represent the factors that influence the blending of the actions of the two controllers, allowing for an appropriate compromise between the individual results of each controller.

To ensure that the function f(e) has only positive values, the form f(e) = e^2 was chosen.

It is highlighted that, when the error is large, the output of the controller multiplied by f(e) is activated more intensely than the other part of the controller. For this reason, in the early stages of the control action, the output of the controller that provides a faster response must be multiplied by f(e).

The switching part of the mechanism tries to identify the greater control effort between the two main components of the controller. Thus, the resulting control function can be of two types:

If $U_{FUZZY} > U_{PID}$ then

$$U_{Hybrid} = f(e) \cdot U_{FUZZY} + (1 - f(e)) \cdot U_{PID} \quad (4)$$

else

$$U_{Hybrid} = (1 - f(e)) \cdot U_{FUZZY} + f(e) \cdot U_{PID} \quad (5)$$

The PID controller was tuned using the continuous-time transfer function of the charging mode and Ziegler-Nichols method for classic PID. The obtained values for the control parameters are as follows: the proportional coefficient (K) is 15.51, the integral time (T_i) is 0.18, and the derivative time (T_d) is 0.05.

4. Simulations and Results

Starting from the technical data of the battery associated with the electric vehicle, specified in Table 3, along with the charging technical characteristics (Koç et al., 2021; Lemian & Bode, 2022), it was computed the expression of the transfer function in the continuous-time domain for the charging mode, as presented below:

$$G_{(s)} = \frac{1.375}{2s+1} e^{-0.09s} \quad (6)$$

Table 3. Parameters of an electric vehicle battery

Serial No.	Parameter Name	Parameter Value
1	Charging voltage	53.8 – 55V
2	Maximum voltage (V_f)	55V
3	Minimum voltage (V_r)	40V
4	Nominal voltage	48V
5	Battery Capacity	50 kWh
6	The nominal primary voltage of the transformer in charging mode	400V
7	Capacity in ampere-hours	125Ah

Figure 9 illustrates the hybrid control model for the automotive battery charging mode, where

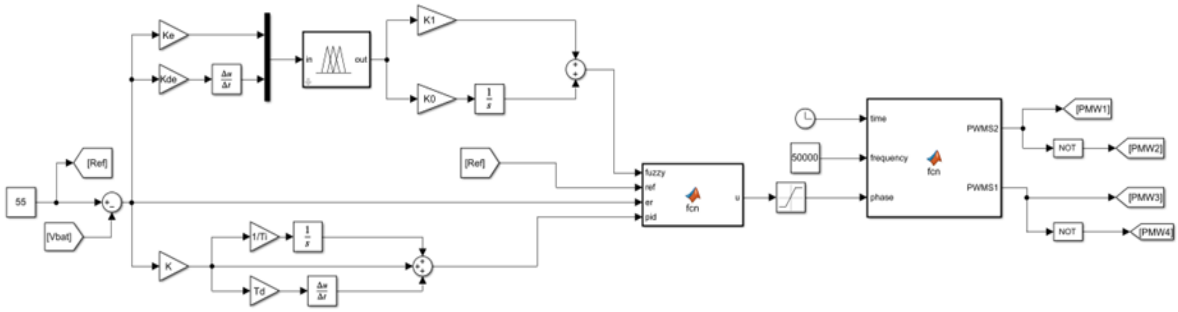

Figure 9. SIMULINK modeling of a hybrid controller for battery charging

two types of controllers are used, namely the traditional PID and the Fuzzy-PID.

In this figure, the presence of the command blending algorithm and the Pulse Width Modulation (PWM) signal modelling algorithm for MOSFET transistors can also be observed.

The hybrid system calculates the variation between the nominal voltage and the actual voltage value, returning a value in the range 0 to 180 degrees, representing the phase shift between the MOSFET transistors Q_1, $Q_2 – Q_3$, Q_4, as it has been defined in Figure 1.

To generate the applied phase shift on the transistors used in the converter, a function was implemented to modify the waveforms of Q_3 and Q_4 to increase/decrease the output voltage.

Furthermore, based on the continuous-time transfer function expressed in equation (7), the gain coefficients for error (K_e), the gain coefficient for error variation (K_{de}), as well as the gain coefficients for the command magnitude (K_0 and K_1) were calculated using equations (8-11).

$$G_{(s)} = \frac{Ke^{-Ls}}{Ts+1} \tag{7}$$

where: K denotes the process gain coefficient, L represents the process dead time, and T represents the process time constant.

$$K_{de} = \min\left(T, \frac{L}{2}\right) \cdot K_e \tag{8}$$

$$K_0 = \frac{1}{K \cdot K_e \cdot \left(\tau_c + \frac{L}{2}\right)} \tag{9}$$

$$K_1 = \max\left(T, \frac{L}{2}\right) \cdot K_0 \tag{10}$$

$$K_e = \frac{1}{r(t_r) - y(t_r)} \tag{11}$$

where *r(tr)* and *y(tr)* represent the reference values and the output values of the system at time *t=tr*. Thus, the following values were obtained: K_e=0.067, K_{de}=0.003, K_0=0.19, and K_1=0.38.

From the graph (Figure 10), it can be observed that the step response resulting from charging the electric vehicle battery with the classical PID controller exhibits a slower response time and significant disturbances, which could have a negative impact on the battery charging mode and its lifespan.

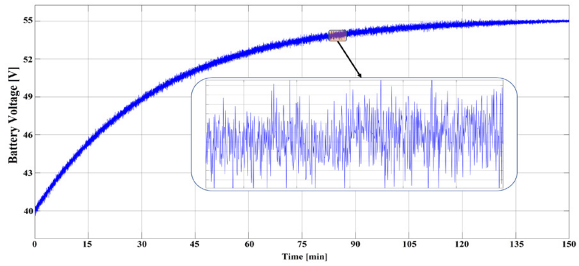

Figure 10. Step response resulting from charging the electric vehicle battery using the PID controller

Figure 11 demonstrates that, by using the hybrid controller consisting of a PID controller and a Fuzzy-PID controller, disturbances have been significantly reduced. Additionally, a reduction in the transient time (10 min) is noticeable, leading to optimal charging mode efficiency. From a practical point of view, it translates into a shorter charging time which is very important for the EV (electric vehicle) user.

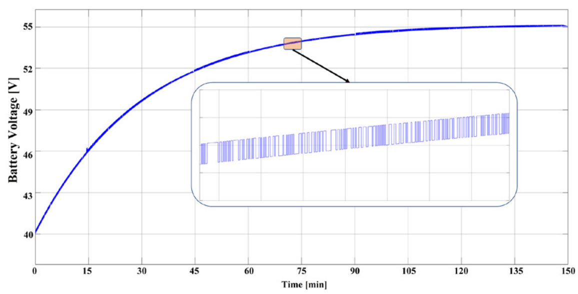

Figure 11. Step response resulting from charging the electric vehicle battery using the hybrid controller

Figure 12 illustrates a comparison between the hybrid controller proposed in the article and a classical PID controller.

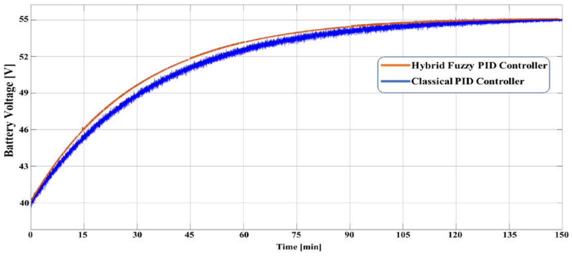

Figure 12. Comparison of the step response resulting from charging the electric vehicle battery using two types of controllers

5. Conclusion

In this study, a charging algorithm for electric vehicle batteries was developed and implemented using a hybrid controller composed of a traditional PID and a Fuzzy-PID controller.

The charging process was powered by energy from a photovoltaic system, and, to convert the voltage from 400 VDC to 48 VDC, modelling and simulation of a full-bridge DC-DC converter with phase-shift control, involving four MOSFET transistors, were required.

Furthermore, a comparison was conducted between the step response of the electric vehicle battery charging mode using a PID controller and the hybrid controller proposed in this article.

The results demonstrated that, by using the hybrid controller, disturbances in the system were significantly reduced, and the response time was improved, leading to efficient charging and an increase in the lifespan of the battery.

The proposal of the hybrid controller brought significant advantages in terms of the performance of the electric vehicle battery charging system, with a positive impact on its operation and durability. The practical impact involves a 10-minute shorter charging time, which brings an advantage for the EV user.

Further work will involve the implementation of an energy management system to support the optimal charging of the vehicle from the photovoltaic system, in the variable environment conditions.

REFERENCES

Alshareef, M. (2022) A New Particle Swarm Optimization with Bat Algorithm Parameter-Based MPPT for Photovoltaic Systems under Partial Shading Conditions. *Studies in Informatics and Control*. 31(4), 53-66. doi: 10.24846/v31i4y202206.

Andronic, C., Fagarasan, I., Arghira, N. & Iliescu, S. S. (2023) Control requirements and efficiency evaluation for PV power plants – a practical approach. In: *2023 24th International Conference on Control Systems and Computer Science (CSCS), 24 – 26 May 2023, Bucharest, Romania*. New Jersey, USA, Institute of Electrical and Electronics Engineers (IEEE). pp. 496-501. doi: 10.1109/CSCS59211.2023.00084.

Baral, K. K., Sahu, P. C., Barisal, A. K. & Mohanty, B. (2023) Combined analysis on AGC and ELD of a hybrid power system with D-WCA designed Gaussian type-2 fuzzy controller. *Evolving Systems.* 14, 263–280. doi: 10.1007/s12530-022-09454-0.

Bhukya, L., Kedika, N. R. & Salkuti, S. R. (2022) Enhanced Maximum Power Point Techniques for Solar Photovoltaic System under Uniform Insolation and Partial Shading Conditions: A Review. *Algorithms.* 15(10), 365. doi: 10.3390/a15100365.

Dobrea, M. A., Arghira, N., Vasluianu, M., Neculoiu, G. & Moldoveanu, A.-M.C. (2021) MPPT techniques application and comparison for photovoltaic panels. In: *2021 23rd International Conference on Control Systems and Computer Science (CSCS), 26 – 28 May 2021, Bucharest, Romania.* New Jersey, USA, Institute of Electrical and Electronics Engineers (IEEE). pp. 386-392. doi: 10.1109/CSCS52396.2021.00070.

Dobrea, M. A., Bichiu, S., Opris, I. & Vasluianu, M. (2020) The Energy Efficiency of a Prosumer in a Photovoltaic System. In: *2020 IEEE 26th International Symposium for Design and Technology in Electronic Packaging (SIITME), 21 – 24 October 2020, Pitesti, Romania.* New Jersey, USA, Institute of Electrical and Electronics Engineers (IEEE). pp. 412-416. doi: 10.1109/SIITME50350.2020.9292256.

Hai, T., Jincheng, Z. & Kengo, M. (2022) An efficient fuzzy-logic based MPPT controller for grid-connected PV systems by farmland fertility optimization algorithm. *Optik.* 267, 4026. doi: 10.1016/j.ijleo.2022.169636.

Kim, H.-Y., Kim, T.-U. & Choi, H.-Y. (2021) A Two-Channel High-Performance DC-DC Converter for Mobile AMOLED Display Based on the PWM–SPWM Dual-Mode Switching Method. *Electronics.* 10(17), 2059. doi: 10.3390/electronics10172059.

Koç, Y., Yaşar, B. & Hacı, B. (2022) Non-isolated high step-up DC/DC converters – An overview. *Alexandria Engineering Journal.* 61(2), 1091-1132. doi: 10.1016/j.aej.2021.06.071.

Leijon, J. & Boström, C. (2022) Charging Electric Vehicles Today and in the Future. *World Electric Vehicle Journal.* 13(8), 139. doi: 10.3390/wevj13080139.

Lemian, D. & Bode, F. (2022) Battery-Supercapacitor Energy Storage Systems for Electrical Vehicles: A Review. *Energies.* 15(15), 5683. doi: 10.3390/en15155683.

Maher, G. M. A., Afida, A., Ammar, H. M. & Taha, S. U. (2023) Optimal fuzzy logic controller based PSO for photovoltaic system. *Energy Reports.* 9(1), 427-434. doi: 10.1016/j.egyr.2022.11.039.

Mendoza-Varela, I. A., Alvarez-Diazcomas, A., Rodriguez-Resendiz, J. & Martinez-Prado, M. A. (2021) Modeling and Control of a Phase-Shifted Full-Bridge Converter for a LiFePO4 Battery Charger. *Electronics.* 10(21), 2568. doi: 10.3390/electronics10212568.

Mohamed, A., Ahmed, M. I., Zuhair, M. A., Adel E.-S. & Ahmed, I. O. (2022) Design and analysis of an efficient photovoltaic energy-powered electric vehicle charging station using perturb and observe MPPT algorithm. *Frontiers in Energy Research.* 10, 969482. doi: 10.3389/fenrg.2022.969482.

Ravipati, V., Mani, S. & Yarlagadda, R. (2021) Efficient Control of Sensorless Hybrid Electric Vehicle Using RBFN Controller. *Studies in Informatics and Control*. 30(4), 87-97. doi: 10.24846/v30i4y202108.

Stamatescu, I., Mihalache, R., Arghira, N., Făgărăşan, I. & Stamatescu, G. (2020) Model for Optimized EVSE Deployment in Dense Urban Areas. In: *IECON 2020 The 46th Annual Conference of the IEEE Industrial Electronics Society, 18 – 21 October 2020, Singapore.* New Jersey, USA, Institute of Electrical and Electronics Engineers (IEEE). pp. 5170-5175. doi: 10.1109/IECON43393.2020.9254960.

Tauš, P., Taušová, M., Sivák, P., Muchová, M. S. & Mihaliková, E. (2020) Parameter Optimization Model Photovoltaic Battery System for Charging Electric Cars. *Energies.* 13(17), 4497. doi: 10.3390/en13174497.

Yao, Y., Kulothungan, G. S. & Krishnamoorthy, H. S. (2022) Improved Circuit Design and Adaptive Burst Mode Control in PSFB Converters for Higher Efficiency Over a Wide Power Range. *IEEE Access.* 10, 9152-9163. doi: 10.1109/ACCESS.2022.3144024.